

Chandra observations of NGC4698: a Seyfert-2 with no absorption

I. Georgantopoulos¹ A. Zezas²

ABSTRACT

We present *Chandra* ACIS-S observations of the enigmatic Seyfert-2 galaxy NGC4698. This object together with several other bona-fide Seyfert-2 galaxies show no absorption in the low spatial resolution *ASCA* data, in contrast to the standard unification models. Our *Chandra* observations of NGC4698 probe directly the nucleus allowing us to check whether nearby sources contaminate the *ASCA* spectrum. Indeed, the *Chandra* observations show that the *ASCA* spectrum is dominated by two nearby AGN. The X-ray flux of NGC4698 is dominated by a nuclear source with luminosity $L_{0.3-8\text{keV}} \sim 10^{39} \text{ erg s}^{-1}$, coincident with the radio nucleus. Its spectrum is well represented by a power-law, $\Gamma \approx 2.2$, obscured by a small column density of $5 \times 10^{20} \text{ cm}^{-2}$ suggesting that NGC4698 is an atypical Seyfert galaxy. On the basis of its low luminosity we then interpret NGC4698 as a Seyfert galaxy which lacks a broad-line region.

Subject headings: galaxies: individual (NGC4698) — galaxies: nuclei — galaxies: active — quasars: general

1. Introduction

Seyfert galaxies are roughly divided in those presenting broad emission lines with $> 1000 \text{ km s}^{-1}$, (Seyfert-1) in their spectra and those having only narrow lines (Seyfert-2). In the standard Active Galactic Nuclei (AGN), unification models (see Antonucci 1993 for a review) the two types of Seyfert galaxies are intrinsically identical with their differences being an orientation effect. In particular, an accretion disk produces the UV continuum which ionizes the surrounding gas: the Broad Line Region (BLR) and the Narrow Line Region (NLR) at distances typically $< 0.1 \text{ pc}$ and $< 100 \text{ pc}$ respectively (e.g. Robson 1996). Then a Seyfert galaxy is classified as type-2 if our line of sight toward the nucleus intercepts

¹Institute of Astronomy & Astrophysics, National Observatory of Athens, Palaia Penteli, 15236, Athens, Greece

²Harvard-Smithsonian Center for Astrophysics, 60 Garden Street, Cambridge, MA02138

an obscuring screen, the so-called torus, which blocks the BLR. There have been several observations supporting these simple unification models. Ground breaking optical studies have detected broad lines in polarized light in NGC1068 demonstrating that a hidden BLR is present in this Seyfert-2 galaxy (Antonucci & Miller 1985). Similarly IR observations showed the existence of obscured BLRs in several Seyfert-2 galaxies (Veilleux et al. 1997). Further evidence supporting the unification models comes from X-ray observations of Seyfert-2 galaxies which show large amounts of obscuration, typically above 10^{23} cm^{-2} , e.g. Smith & Done (1996), Turner et al. (1997).

However, some questions arise regarding whether the unification models can be applied to all Seyferts. Polarimetry studies have shown that a significant fraction of Seyfert-2 galaxies appear to lack a hidden BLR (Moran et al. 2000, Tran 2001). A correlation with luminosity is observed in the sense that the less luminous Seyfert nuclei are those missing a BLR (Tran 2001, Lumsden & Alexander 2001). Moreover, *ASCA* observations of some Seyfert-2 galaxies show that these do not present intrinsic X-ray absorption: NGC3147, Ptak et al. (1996), NGC7590, Bassani et al. (1999), NGC4698, Pappa et al. (2001). Recently Panessa & Bassani (2002) added several more candidates in this list. One has to be cautious in identifying candidate ‘unabsorbed Seyfert-2’ as the optical spectroscopy may not be of sufficient quality in order to classify them as bona-fide Seyfert-2 galaxies. Furthermore, some of the objects may be Compton thick i.e. the transmitted component below 10 keV is completely absorbed. Then in the *ASCA* 1-10 keV band we would observe only the scattered, *unabsorbed* component. The lack of a strong Fe line at 6.4 keV as well as the high ratio of the broad band hard X-ray over the [OIII] line emission (the latter comes from the NLR and thus represents an isotropic measurement of the luminosity; e.g. Alonso-Herrero et al. 1997) can be used to discriminate against the Compton thick model. Finally, the *ASCA* Point Spread Function is large (3 arcmin Half-Power Diameter) and hence the observed X-ray emission may be contaminated by other nearby sources, or the integrated emission of the host galaxy. This confusion problem is particularly important in the Low Luminosity Seyferts where the energy output of a few strong Ultra-Luminous X-ray (ULX) sources may rival the luminosity of the nucleus (e.g. Ho et al. 2001).

Here, we discuss *Chandra* observations of NGC4698. NGC4698, at a distance of 16.8 Mpc, belongs to the spectroscopic sample of nearby galaxies of Ho, Filippenko & Sargent (1997). The excellent quality nuclear spectra obtained (2×4 arcsec slit) make the Seyfert-2 classification for this galaxy highly certain. Pappa et al. (2001) observed NGC4698 with *ASCA*. Their best-fit model is an unobscured ($9 \pm 4 \times 10^{20} \text{ cm}^{-2}$) power-law $\Gamma = 1.91^{+0.12}_{-0.10}$ with a luminosity of $L_{2-10\text{keV}} \approx 2 \times 10^{40} \text{ erg s}^{-1}$. No FeK line is detected with the upper limit on equivalent width being $\sim 0.4 \text{ keV}$ at the 90% confidence level. The absence of a strong FeK line as well as the high value of the $f_x/f_{[\text{OIII}]}$ ratio suggested that NGC4698 is not a

Compton thick object. However, the spectrum measured by *ASCA* may be contaminated by other nearby sources which mask the true nuclear emission. The excellent spatial resolution of *Chandra* allows us to obtain a direct view of the nuclear region without any confusion problems.

2. Observations and Data Reduction

NGC4698 was observed on 2002-June-16 (OBSID 3008), using the Advanced CCD Imaging Spectrometer, ACIS-S, onboard *Chandra* (Weisskopf et al. 1996). The back-illuminated ACIS-S3 CCD was on the aimpoint, providing a spatial resolution of $0.5''$ and minimizing Charge Transfer Inefficiency (CTI) problems. In order to minimize pile-up the observation was performed in 1/2-subarray mode. In this mode the field of view is $4.1' \times 8.3'$ which covers the whole galaxy. We use the type-2 event file (including only grades 0,2,3,4 and 6) provided by the standard pipeline processing after discarding periods of high background. The resulting exposure time is 29726 sec. Images, spectra and lightcurves have been created using the *CIAO* v2.2 software. The imaging and timing analysis were performed using the *SHERPA* software. For the spectral fitting we use the *XSPEC* v11 software package.

3. Analysis

3.1. Imaging

Three strong sources are detected by *Chandra* in the vicinity of NGC4698. The detected sources together with the *ASCA* GIS contours are shown in Fig.1. The cross gives the position of the central source which is spatially coincident with the optical center of the galaxy and therefore we identify it as the nucleus. The nuclear source is also coincident with a faint radio source detected by Ho & Ulvestad (2001) at equatorial coordinates $\alpha = 12^h48^m22^s.92$ $\delta = +08^\circ29'14''.5$ (J2000). Its radio flux density was 0.23 mJy at 6 cm corresponding to a radio power of $\sim 10^{19}$ W Hz $^{-1}$. RXJ1248.4+0831 (source 1, on Fig. 1), originally detected in the *ROSAT* All-Sky-Survey was identified as a redshift $z=0.12$ AGN (Bade et al. 1998). J124825.9+083021 is a radio source (denoted as source 2 on Fig.1) detected by Ho & Ulvestad (2001), having a flux density of 0.8 mJy at 6 cm. Recently, Foschini et al. (2002) identified this source as a probable BL Lac at a redshift of $z=0.43$. Since the latter sources are ~ 6 and ~ 4 times brighter than the nucleus of NGC4698 in the 0.3-8.0 keV band (Table 1), the *ASCA* spectrum is dominated by them *instead of the NGC4698 nucleus*. Although, the *ASCA* data cannot give an uncontaminated spectrum of the nucleus due to

their limited spatial resolution, Pappa et al. (2001) assumed that all the X-ray emission observed by ASCA arises from NGC 4698 and failed to discuss the possible contamination from the nearby *ROSAT* source.

The X-ray luminosity of the nuclear source is relatively low ($L_X \sim 10^{39}$ erg s $^{-1}$; 0.3–8.0 keV), leaving open the possibility that it could be associated with a ULX, (see Ward 2002 for a recent review). Nevertheless, the fact that the nuclear X-ray source is coincident with the radio and optical nucleus suggests that our source is most probably associated with the supermassive black hole at the center of NGC4698. Moreover, the ratio of the X-ray to radio luminosity (see Terashima & Wilson 2003 for the definition) of the nuclear source in NGC4698 is an order of magnitude lower than in the case of the ULX in NGC5408, the only extragalactic X-ray binary emitting at ULX levels identified with a radio source (Kaaret et al. 2003). The value of the above ratio ($\sim 10^{-6}$) puts NGC4698 clearly in the regime of radio quiet AGN.

Seven more X-ray sources are detected within or around NGC4698 down to $\sim 2 \times 10^{-15}$ erg cm $^{-2}$ s $^{-1}$. The details of all the above sources are given in Table 1. We give the name, equatorial coordinates (J2000), counts, the absorbed flux and luminosity (all in the total 0.3–8 keV band) in columns 1, 2, 3, 4 and 5 respectively. Counts were extracted from a 4 pixel (2 arcsec) radius circle. For the seven off-nuclear sources in NGC4698, the conversion from count rate to flux was performed assuming a power-law spectrum of $\Gamma = 1.9$, consistent with the spectrum of Low Mass X-ray Binaries in nearby galaxies e.g. Prestwich et al. (2003). We further assume that the above spectrum is only absorbed by the Galactic column density, $N_H = 2 \times 10^{20}$ cm $^{-2}$, (Dickey & Lockman 1990). For the nucleus, RXJ1248.4+0831 and J124825.9+083021 we used the spectra derived from the spectral fits below. Luminosities are estimated assuming $H_0 = 75$ km s $^{-1}$ Mpc $^{-1}$, $q_0 = 0.5$ and $\Lambda = 0$.

We have fitted the two-dimensional spatial profile of the nuclear source with the *SHERPA* software. We use a radius of 2 arcsec for our fit. Fitting a Gaussian profile, we obtain a FWHM of 1.58 ± 0.18 pixels. Given that the nominal Point Spread Function (PSF) is undersampled by the pixels of the ACIS camera (FWHM $_{PSF} \sim 0.5''$ at 1.5 keV, compared to a pixel size of $0.49''$) we consider the probability of any extension very marginal.

3.2. Spectral Fitting

We obtained spectra for the three brightest sources, for which is possible to perform any spectral analysis, using an extraction radius of 2 arcsec. Background regions are taken from source free regions on the same chip. Note however, that the background contribution is

practically negligible with about 1 count in the above extraction radius. We group the data so that there are at least 15 counts per bin. The quoted errors to the best fitting spectral parameters correspond to the 90% confidence level for one interesting parameter. We discard data below 0.3 keV due to the low response as well as calibration uncertainties. In order to take into account the degradation of the ACIS quantum efficiency in low energies, we used the *ACISABS* model in the spectral fitting³. We present spectral fits for the following sources:

The nucleus of NGC4698 A single power-law fit gives a good fit to the data ($\chi^2_\nu = 5.8/9$). The column density is $N_H = 5^{+0.7}_{-0.5} \times 10^{20} \text{cm}^{-2}$ a factor of two above the Galactic value ($2.0 \times 10^{20} \text{cm}^{-2}$; Dickey & Lockman, 1990). This is much lower than the column densities encountered in typical Seyfert-2 galaxies (eg Smith & Done 1996, Turner et al. 1997). The photon index is $\Gamma = 2.18^{+0.28}_{-0.44}$. Unfortunately our data are not of sufficient quality to check for the presence of an FeK line at 6.4 keV. The spectrum of the source together with the residuals from the best-fit power law model are given in Fig. 2.

RXJ1248.4+0831 The single power-law fit yields a relatively poor fit to the data ($\chi^2 = 75.8/55$). The photon index is $\Gamma \sim 1.7$ while the column density is constrained to be less than $1.0 \times 10^{20} \text{cm}^{-2}$. The photon index is characteristic of those of Seyfert-1 nuclei (Nandra & Pounds 1994). When we add a thermal Raymond-Smith component (Raymond & Smith 1977), absorbed only by the Galactic column, the fit is significantly improved ($\chi^2 = 64.5/55$). The temperature of the thermal component is $kT \sim 0.2 \text{ keV}$. Then, the photon index becomes $\Gamma = 1.49^{+0.12}_{-0.12}$. The luminosity of the thermal component is $L_{0.3-2\text{keV}} \sim 6 \times 10^{41} \text{ erg s}^{-1}$ or about 20 per cent of the total luminosity in this band.

J124825.9+083021 A single power-law fit yields $\chi^2_\nu = 40.0/38$. The column density is consistent with the Galactic ($N_H < 8 \times 10^{20} \text{ cm}^{-2}$) while the photon index is 2.02 ± 0.11 . The *Chandra* spectrum in very good agreement with that obtained by Foschini et al. (2002). These authors find $\Gamma = 2.0 \pm 0.2$ with $\chi^2_\nu = 18.3/24$ using *XMM-Newton* data. Note that the X-ray flux has increased by less than a factor of two between the *Chandra* and the *XMM-Newton* observation (obtained at 16/12/2001).

4. Discussion

Previous ‘large-beam’ observations, mostly performed with *ASCA* and *BeppoSAX*, have shown the presence of a population of low luminosity Seyfert-2 galaxies with no absorption

³http://asc.harvard.edu/cal/Acis/Cal_prods/qeDeg

in their X-ray spectra (e.g. Panessa & Bassani 2002). However, the low X-ray spatial resolution casts doubt on whether the X-ray spectra observed are those of the nuclei. The problem is more acute in the case of low luminosity nuclei where the nuclear flux can be easily outshined by adjacent bright sources. Indeed, the *Chandra* observation of NGC4698 reveals that the *ASCA* data *did not probe the nucleus of NGC4698*. The X-ray flux in the *ASCA* beam is dominated by two nearby sources while the contribution of the NGC4698 nucleus is very small, ~ 10 per cent of the total 0.3-8 keV *ASCA* flux. We find that several other sources in the galaxy contribute about 40 per cent of the total galactic flux. Given their luminosity ($L_x \sim 5 \times 10^{37} - 2 \times 10^{38}$ erg s $^{-1}$), these are most probably associated with X-ray binaries. However, accidentally, the spectrum of the nucleus again appears to show no absorption having $N_H = 5 \times 10^{20}$ cm $^{-2}$, only a factor of two above the Galactic column density. However, as the nuclear flux measured by *ASCA* is erroneous, we need to assess again whether NGC4698 is a Compton thick source. Using the new *Chandra* 2-10 keV flux, the $f_{2-10\text{keV}}/f_{[\text{OIII}]}$ ratio is ~ 1 . This value is still in the regime of the Compton thin AGN (Bassani et al. 1999). Although the FeK α line could provide additional information, the poor photon statistics of NGC4698 do not allow us to set any constraints based on this diagnostic tool: no photons have been detected above 5 keV. Nevertheless, we note that Compton thick Seyferts appear to have a flat spectrum $\Gamma \sim 1$ in the 2-10 keV band (e.g. Matt et al. 1996). This can be explained as the hard reflection component from the back-side of the torus dominates the observed spectrum in the 2-10 keV band over the reflected power-law spectrum. A pure reflected $\Gamma = 1.9$ spectrum, in principle, could be obtained in the rare case where the orientation is such that the torus is exactly edge-on so that the hard reflection component is completely hidden from view. Therefore, the *Chandra* spectrum rather adds evidence against the Compton thick scenario.

To our knowledge, NGC4698 is the second Seyfert-2 galaxy from the Ho et al. (1997) sample with no X-ray absorption as demonstrated by *Chandra* observations. The other example is NGC3147: a recent snapshot *Chandra* observation of this galaxy (Terashima & Wilson 2002), clearly shows that the nucleus is unabsorbed in agreement with the *ASCA* spectrum. In particular, the *Chandra* spectrum yields $\Gamma = 1.79^{+0.17}_{-0.09}$ with $N_H \sim 1.5 \times 10^{21}$ cm $^{-2}$ ($L_{2-10\text{keV}} \sim 8 \times 10^{41}$ erg s $^{-1}$). No FeK line is detected at 6.4 keV with *Chandra*. Moreover, the variability observed between the *Chandra* and the *ASCA* epoch strongly suggests that the X-ray emission is not scattered radiation from an extended region.

A model where the X-rays come through unabsorbed while the BLR is attenuated is rather unlikely. A warm absorber retaining dust could in principle attenuate the optical radiation while leaving intact the X-rays. Still, a warm absorber would imprint strong oxygen absorption features in the X-ray spectrum below 1 keV. Such absorption edges have not been seen in the spectrum of NGC3147, while it is impossible to check for such features

in the much poorer quality spectrum of NGC4698. Another possible explanation for the lack of X-ray absorption in NGC4698 and NGC3147 is that we are simply viewing a Seyfert-1 nucleus which does not have a BLR. This is the pure Seyfert-2 model of Tran (1995). Recent models (eg Nicastro 2000, Laor 2003) suggest that a BLR cannot exist at low accretion rates. In particular, Nicastro (2000) (see also Nicastro, Martocchia & Matt 2003) advocate a model where the BLR is associated with a wind coming from the accretion disk. In this model the width of the broad lines depends on the accretion rate in the sense that AGNs accreting in a *much lower rate than their Eddington limit* ($< 1 - 4 \times 10^{-3} \times M_{Edd}$) should possess no BLR. Note however, that the exact accretion rate limit depends on the accretion disk physics. Therefore it may not be surprising that there are a few cases of low accretion rate AGN with a BLR (see the discussion in Laor 2003).

The accretion rate in the case of NGC4698 can be easily estimated as follows. The observed velocity dispersion is 169 km s^{-1} (McElroy 1995; Corsini et al. 1999, estimate a somewhat lower value of 134 km s^{-1}). Then from the relation between the black hole mass and the velocity dispersion (e.g. Gebhardt et al. 2000), we find a black-hole mass of $M_{BH} \sim 2 - 8 \times 10^7 M_{\odot}$. In this estimate we take into account both the quoted errors in the relation of Gebhardt et al. (2000) as well as the variations between the different measurements of the velocity dispersion. Hence, the predicted Eddington luminosity is $\sim 3 - 10 \times 10^{45} \text{ erg s}^{-1}$. We estimate the bolometric luminosity by integrating the measured X-ray luminosity down to $100\mu\text{m}$ using a power-law energy spectrum of slope $\alpha = 1$, characteristic of the broad-band AGN spectrum (e.g. Robson 1996). This yields $L_{BOL} = 4 \times 10^{39} \text{ erg s}^{-1}$. Note however, that if we use instead the relation between the bolometric luminosity and the narrow $H\alpha$ luminosity (see Laor 2003) we obtain $L_{BOL} = 4 \times 10^{40} \text{ erg s}^{-1}$. Hence $L_{BOL}/L_{EDD} \sim 4 \times 10^{-7} - 1 \times 10^{-5}$. In the case of NGC3147 we estimate a central mass of $3 - 5 \times 10^8 M_{\odot}$, from the measured bulge velocity dispersion, 268 km s^{-1} , (McElroy 1995). Therefore the predicted Eddington Luminosity is $L_{EDD} = 4 - 6 \times 10^{46} \text{ erg s}^{-1}$. Extrapolation of the X-ray emission down to $100\mu\text{m}$, using $\alpha = 1$ gives $L_{BOL} = 3 \times 10^{42} \text{ erg s}^{-1}$; the narrow $H\alpha$ luminosity gives instead $L_{BOL} = 3 \times 10^{41} \text{ erg s}^{-1}$. Hence, $L_{BOL}/L_{EDD} \sim 5 \times 10^{-6} - 1 \times 10^{-4}$. According to the theoretical models discussed earlier, these low accretion rates are totally consistent with an absent BLR.

Unfortunately, there are no polarimetry data for NGC4698 or NGC3147 in order to search for the presence of a hidden BLR and therefore to test directly the above model. In the case of NGC7590, which also has a low column density, where such data are available (Heisler, Lumsden & Bailey 1997) no BLR is detected. Tran et al. (2001) find that the Seyferts with no hidden BLR are those with the lowest luminosity. Therefore, it is possible that there is a link between the Seyfert-2 galaxies which present no absorption in their X-ray spectrum with those which lack a hidden BLR. However, in the samples of Tran et al. (2001)

and Lumsden & Alexander (2001) there are a few examples of Seyfert-2 galaxies without a BLR but with large amounts of X-ray absorption. This could be simply explained according to an orientation effect in the standard unification model framework. Assuming that all AGN with low accretion rate do possess a torus but have no BLR, objects like NGC4698 which present no X-ray absorption must be viewed face-on while the ones with absorption are viewed edge-on.

In conclusion, *Chandra* observations of NGC4698 (and NGC3147) confirm that these galaxies host nuclei which present very little X-ray absorption, although they are classified as Seyfert-2 by optical spectroscopy. This is in disagreement with the standard unification models where a dense obscuring screen is believed to block the BLR and to absorb the soft X-ray radiation. The most straightforward explanation is that NGC4698 lacks a BLR. This could be in line with theoretical models where the BLR clouds are not formed at low accretion rates, and explains the low absorbing column density in other low-luminosity AGNs classified as type-2 on the basis of their optical spectra.

We thank Fabrizio Nicastro for many useful comments. This work has been supported by the NASA grant NAG-G02-3127X.

REFERENCES

- Alonso-Herrero, A., Ward, M.J., Kotilainen, J.K., 1997, MNRAS, 288, 977
- Antonucci, R.R.J., 1993, ARA&A, 31, 473
- Antonucci, R.R.J. & Miller, J.S., 1985, ApJ, 297, 621
- Bade, N., et al., 1998, A&A, 127, 145
- Bassani, L., Dadina, M., Maiolino, R., Salvati, M., Risaliti, G., della Ceca, R., Matt, G., Zamorani, G. 1999, ApJS, 121, 473
- Corsini, E.M., et al. 1999, A&A, 342, 671
- Dickey, J.M., Lockman, F.J., 1990, ARA&A, 28, 215
- Foschini, L. et al. 2002, A&A, 396, 787
- Gebhardt, K. et al., 2000, ApJ, 539, L13
- Heisler, C.A., Lumsden, S.L., Bailey, J.A., 1997, Nat, 385, 700
- Ho, L.C., Filippenko, A.V., & Sargent, W.L.W., 1997, ApJS, 112, 315
- Ho, L.C. et al., 2001, ApJ, 549, L51

- Ho, L.C., & Ulvestad, J.S., 2001, ApJS, 133, 77
- Laor, A., 2003, ApJ, in press, astro-ph/032541
- Lumsden, S.L. & Alexander, D.M., 2001, MNRAS, 328, L32
- Matt, G., et al. 1996, MNRAS, 281, L69
- McElroy, D.B., 1995, ApJS, 100, 105
- Nandra, K. & Pounds, K.A., 1994, MNRAS, 268, 405
- Nicastro, F., 2000, ApJ, 530, L65
- Nicastro, F., Martocchia, A., Matt, G., 2003, ApJ, submitted
- Panessa, F., & Bassani, L., 2002, A&A, 394, 435
- Pappa, A., Georgantopoulos, I., Stewart, G.C., Zezas, A., 2001, MNRAS, 326, 995
- Prestwich, A.H., Irwin, J.A., Kilgard, R.E., Krauss, M.I., Zezas, A., Primini, F., Kaaret, P. 2003, ApJ, in press, astro-ph/0206127
- Ptak, A., Yaqoob, T., Serlemitsos, P.J., Kunieda, H., Terashima, Y., ApJ, 1996, 459, 542
- Raymond, J.C., & Smith B.W., 1977, ApJS, 35, 419
- Reeves, J.N., & Turner, M.J.L., 2000, MNRAS, 316, 234
- Robson, I., 1996, in 'Active Galactic Nuclei', Wiley-Praxis
- Smith, D.A., & Done, C., 1996, MNRAS, 280, 355
- Terashima, Y., & Wilson, A.S., 2003, ApJ, 583, 145
- Tran, H.D., 1995, ApJ, 440, 597
- Tran, H.D., 2001, ApJ, 554, L19
- Turner, T.J., George, I.M., Nandra, K., Mushotzky, R.F. 1997, ApJ, 488, 164
- Veilleux, S., Goodrich, R.W., Hill, G.J., 1997, ApJ, 477, 631
- Ward, M.J., 2002, Phil. Trans. R. Soc. London, 360, 1991
- Weisskopf, M.C., O'dell, S.L., van Speybroeck, Leon P., 1996, SPIE, 2805, 2

Table 1: The detected X-ray sources

Name	Equatorial Coordinates (J2000)	Counts	logf (0.3-8 keV) erg cm ⁻² s ⁻¹	logL (0.3-8 keV) erg s ⁻¹
Nucleus	12 48 22.9 +08 29 15	168	-13.5	39.0
CXUJ124823.6+082844	12 48 23.6 +08 28 44	28	-14.3	38.2
CXUJ124823.3+082901	12 48 23.3 +08 29 01	10	-14.8	37.7
CXUJ124823.2+082915	12 48 23.2 +08 29 15	14	-14.6	37.9
CXUJ124822.2+082917	12 48 22.2 +08 29 17	24	-14.4	38.1
CXUJ124822.2+082926	12 48 22.2 +08 29 26	14	-14.6	37.9
CXUJ124824.3+082754	12 48 24.3 +08 27 54	12	-14.7	37.8
CXUJ124826.4+082955	12 48 26.4 +08 29 55	14	-14.6	37.9
RXJ1248.4+0831	12 48 28.4 +08 31 12	986	-12.6	42.8
J124825.9+083021	12 48 25.9 +08 30 21	699	-12.8	43.8

Table 2: Power-law Spectral fits

Source	N _H (10 ²⁰ cm ⁻²)	Γ	χ ²
NGC4698 nucleus	5 ^{+0.7} _{-0.5}	2.18 ^{+0.28} _{-0.44}	5.8/9
RXJ1248.4+0831	< 1	1.67 ^{+0.09} _{-0.09}	75.8/55
J124825.9+083021	4 ⁺⁴ ₋₄	2.02 ^{+0.11} _{-0.11}	40.0/38

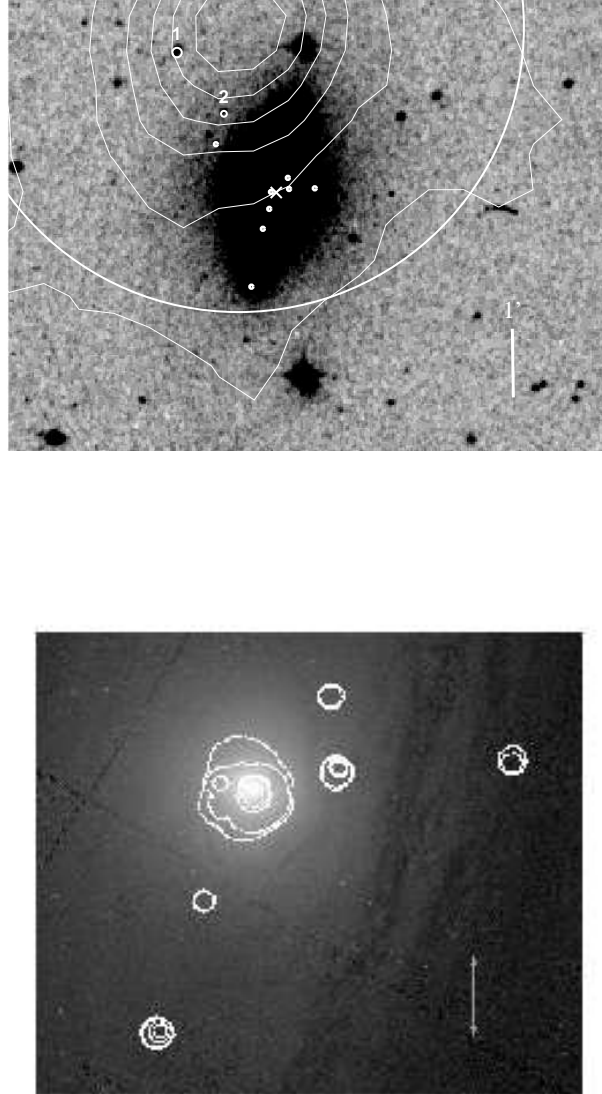


Fig. 1.— Upper: The sources detected in the *Chandra* image overlaid on the Digital Sky Survey image. Sources 1 and 2 denote RXJ1248.4+0831 and the radio source J124825.9+08302 respectively. The white dots correspond to the 7 sources which are probably associated with the galaxy, given in table 1. The cross denotes the most luminous source in NGC4698 which coincides with the optical and the radio nucleus. The contours from the *ASCA* GIS observation are also overlaid. The circle (4 arcmin radius) corresponds to the *ASCA* extraction radius used by Pappa et al. (2001). The line corresponds to 1 arcmin. Lower: The *Chandra* 0.3-8 keV contours overlaid on an *HST* WFPC2 (F606W filter) image. The line corresponds to 10 arcsec.

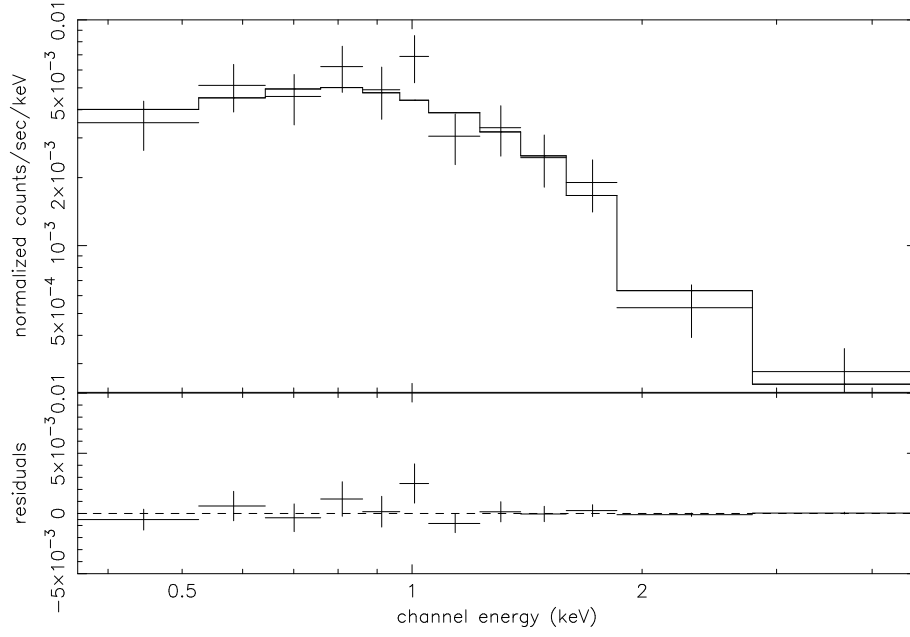


Fig. 2.— The spectrum of the nuclear source in NGC4698 together with the best fit power-law model (upper panel). In the lower panel we plot the residuals of the data from the best fit model.